

# We are IntechOpen, the world's leading publisher of Open Access books Built by scientists, for scientists

6,900

Open access books available

185,000

International authors and editors

200M

Downloads

Our authors are among the

154

Countries delivered to

TOP 1%

most cited scientists

12.2%

Contributors from top 500 universities



WEB OF SCIENCE™

Selection of our books indexed in the Book Citation Index  
in Web of Science™ Core Collection (BKCI)

Interested in publishing with us?  
Contact [book.department@intechopen.com](mailto:book.department@intechopen.com)

Numbers displayed above are based on latest data collected.  
For more information visit [www.intechopen.com](http://www.intechopen.com)



# Structural Design of a Dynamic Model of the Battery for State of Charge Estimation

Frédéric Coupan, Ahmed Abbas, Idris Sadli,  
Isabelle Marie Joseph and Henri Clergeot  
*UMR ESPACE-DEV, Université des Antilles et de la Guyane  
Guyane Française*

## 1. Introduction

For a standard interconnected electrical power network, the problem of optimal management of production arises from randomness of users demand. When using renewable energies, an additional critical problem is that the resource itself is random. The difficulty is still more pregnant when dealing with small isolated production networks, in locations where photovoltaic systems or wind generators should be a promising solution. To resolve the difficulties induced by intermittent production or consumption, these systems must make a consistent use of the energy storage. For example, in the case of an individual photovoltaic system, storage is essential to the scale of at least 24h, in order to overcome the daily fluctuations.

Among the various methods used to store electrical energy, electrochemical batteries constitute the most readily available, with good performance and a reasonable cost (Riffonneau et al., 2008). Renewable Energies are concerned by stationary storage, for which lead acid batteries are a good choice. Despite decades of use and its apparent simplicity, the battery maintains a complex and poorly understood dynamical behavior. Moreover, possible degradation of the battery is largely related to poor control of periods of deep discharge or full load with gassing. For efficient use of this device, a detailed knowledge of operation, and thus a good electrochemical modeling, is essential. Otherwise, it could constitute the most fragile element in a photovoltaic or wind systems because of premature aging resulting in a loss of capacity or a failure risk (Garche et al., 1997). A lot has been done in the domain of batteries modeling from two opposite ways.

On the one hand, a purely phenomenological approach has been developed by engineers. In particular, very valuable tests are commonly performed using battery cycling with constant charge and discharge currents. In particular, there appears a reduction of the effective capacity when the cycling current increases (Peucker's law (Manwell Jams, 2003)). These results may have direct application for charge monitoring in systems with alternate charging and discharging sequences (for instance traction vehicles); unfortunately, they do not apply to wind turbines or photovoltaic applications subject to random electrical current variations.

On the other hand, extensive physical studies have been made by electrochemists concerning the physics of electrochemical cells. Descriptions of the cell behavior have been

proposed in terms of equivalent electrical circuits (Bard, 2000). In particular, associated to diffusion phenomenon, the Warburg impedance  $Z_w$  has been introduced, involving integration with a non integer order. In Laplace notation (where  $p$  denotes the equivalent derivation operator) the Warburg impedance has the form:  $Z_w = A p^{-1/2}$ . In a previous communication, we demonstrated that the effective cell capacity reduction described by Peucker's law may be connected to the step response associated to the Warburg impedance (Marie-Joseph et al., 2004).

Anyway, some midway solution must obviously be found between underlying fundamental physics and the need of the engineers for a computationally efficient simplified model.

In this chapter, we discuss the major processes resulting in a voltage drop that occurs during a redox reaction sitting in storage electrochemical. The phenomena of diffusion/storage and activation are identified as the main factors for the voltage drop in the batteries (Esperilla et al., 2007). These phenomena occur when the battery is subjected to an electric current, which is to say when there is mass transport in electrochemical interface; they are called faradic phenomena. Focusing particularly on transport mechanism of carriers in the battery, we observed strong similarities between electrochemical interfaces and PN junction diodes (Coupan et al., 2010). Based on the approximation of the physics of semiconductor PN junction, we propose a physical analysis coupled to experimental investigation.

Along these lines, in this chapter, we introduce a dynamical model of the battery, which explains in terms of a simplified equivalent circuit how the total stored charge is distributed along a cascade of individual elements, with increasing availability time delays. This explains why short cycling makes use only of the closer elements in the chain. It opens the way to a wise design of systems combining short delay storage (for instance super-capacities) and conventional batteries used for long term full range cycling.

## 2. Analysis methodology

At steady state (without current), according to the electrical charges of the reactants in the redox reaction, the chemical potential gradient across the interface may be balanced by an electrical potential gradient. This electric field, integrated across the interface, results in the equilibrium potential given by the Nernst relationship (Marie-Joseph, 2003).

When a current is applied to the electrochemical cell, the electronic flow in the metal terminals corresponds to an ionic flow, in proportion defined by the redox reaction stoichiometry at the electrolyte interface. Corresponding carriers which are present in the electrolyte can then move either under the effect of an electrical potential gradient (migration) or the effect a concentration gradient (diffusion). Occasionally, electrolyte transport by convection may also be of influence (Linden et al., 2001). This movement of carriers causes a change in battery voltage compared to the steady state potential, called over-potential. Note that it is a nonlinear function of the current, depending not only on the present value of the current but on its past variations: it is termed a dynamical non linear relationship. The phenomena responsible for this over-potential involve a number of different and complex processes that overlap each other: that is to say, the kinetics of electron transfers, mass transfers, but also ohmic effect and other non-faradic effects. In this study, we focus on the phenomena of diffusion/storage and activation.

- The diffusion/storage overvoltage is connected to variation of the ionic concentrations in the electrolyte: average value related to the state of charge, and gradient related variation at the interface in presence of current. However this phenomenon always

appears in agreement with the Nernst equation. We propose a linearisation by inversion of this relation and a dynamical model drawing from the analogy of diffusion equation with a capacitive transmission line. Diffusion phenomena predominate for response times ranging from  $10^3$  to  $10^5$ s.

- The activation overvoltage may be related to injection of sulfate ions in the oxide film at the surface of electrodes. These constitute solid electrolytes no longer governed by Boltzmann but by Fermi-Dirac statistics. There are strong similarities which the injection of minority carriers in PN junctions. In the literature, this phenomenon is usually described by the semi empirical Butler-Volmer relation. We propose a dynamical model drawn from the charge driven model of PN diodes, with given relaxation time (typically in the order of some  $10^2$  s).
- Full description of the battery includes conventional circuit modeling of non faradic effects. This is taken into account by an RC “input cell” including plates electrostatic capacitance, Ohmic resistance and the plates double layer capacitances, with typical time constants between 1s and 100s. High frequency models may include inductive effects (Blanke et al, 2005).

### 3. Input cell and diffusion voltage for lead acid batteries

#### 3.1 Input impedance cell

With a simplified assumption of symmetrical electrochemical impedance for the electrodes (denoted  $Z'/2$ ), we can infer equivalent circuit of fig 1-a,  $\gamma$  being an inter-plates capacitance,  $R$  the electrolyte resistance and  $2C_0$  the double layer capacitance of the interface. The corresponding reduced input circuit is given fig 1-b.

Elements of the input cell are easily identified experimentally at small operating currents and high enough frequencies. Due to the activation threshold, impedance  $Z'$  is quite high at low current, so that the double layer impedance  $C_0$  dominates for frequencies greater than about 0.1 Hz.

Once the elements of the cell are known, current and voltage may easily be corrected for. In the following, we are interested only in the internal electrochemical impedance  $Z'$ .

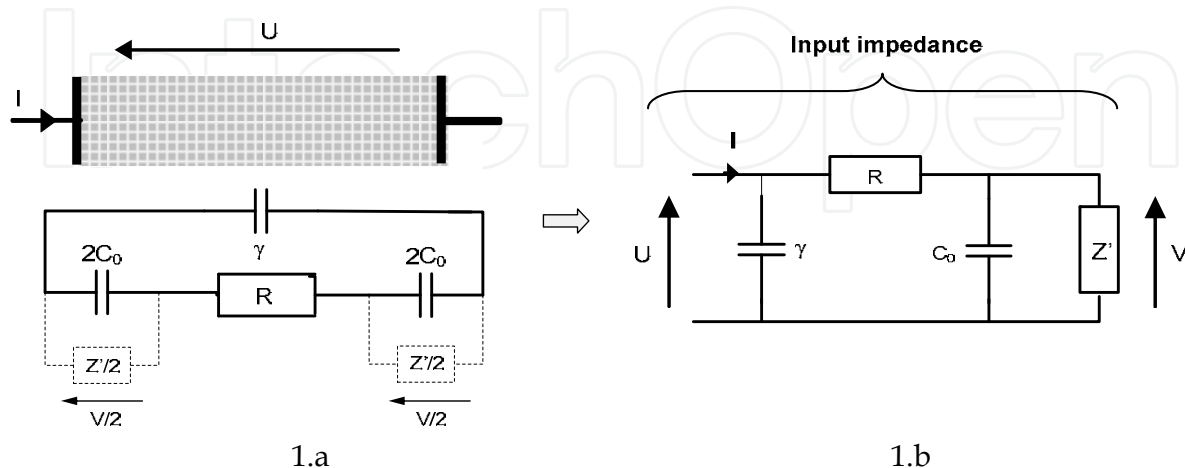


Fig. 1. Input impedance cell (simplified symmetric plates model)

### 3.2 Diffusion overvoltage

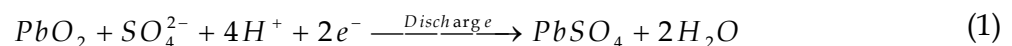
For the sake of clarity, a good part of the analysis will be carried in the stationary case, corresponding to constant current. We use a one dimensional battery model, the variable being the abscissa  $z$  between the negative ( $z=0$ ) and the positive plate ( $z=L$ ). Results are then extended with a constant cross section  $S$ , to the general dynamical case, including time dependency.

#### 3.2.1 Constant current analysis

##### 3.2.1.1 General presentation

During the discharge of the lead acid battery, sulfate ions are “swallowed” by both electrodes according to chemical reactions:

Positive electrode:



Negative electrode:

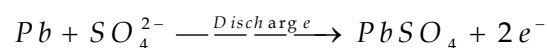


Figure 2 illustrates the transport of ions along axis  $Oz$  associated with the two half-reactions at the electrodes (inter-electrode distance  $L$ ):

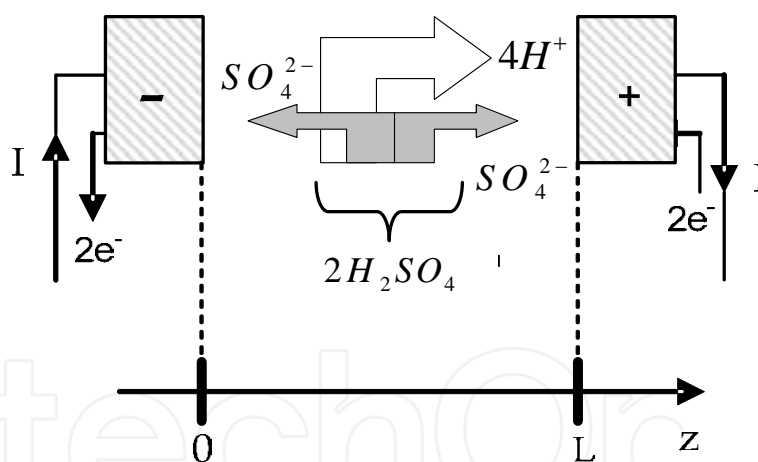


Fig. 2. Battery operation: case of discharge

So, two types of ions are responsible for current transport through the electrolyte. Those are sulfate ions (subscript S) and hydrogen ions (subscript H). In terms of currents:

$$I(z) = I_H(z) + I_S(z) \quad (2a)$$

Let  $S$  be the section area between the plates (constant for a one dimensional model). The same relation holds in terms of current densities:

$$J(z) = \frac{I}{S} = J_H(z) + J_S(z) \quad (2b)$$

In the electrolyte, as can be seen in figure 2, there is an inversion of the sulfate ions flow along the  $z$  axis. More precisely according to the simultaneous equations (2), we obtain the boundary conditions at the electrodes:

$$I_S(0)=I \text{ and } I_H(0) = 0 \quad (3a)$$

$$I_S(L) = -I \text{ and } I_H(L) = 2I \quad (3b)$$

As it will be seen in section 3.2 the constant current case corresponds to a stationary solution of the dynamical case with  $\partial^2 I / \partial z^2 = 0$ , which implies a linear variation of the current between the given limits. The profile of currents  $I_S(z)$  and  $I_H(z)$  is then obtained according to Figure 3:

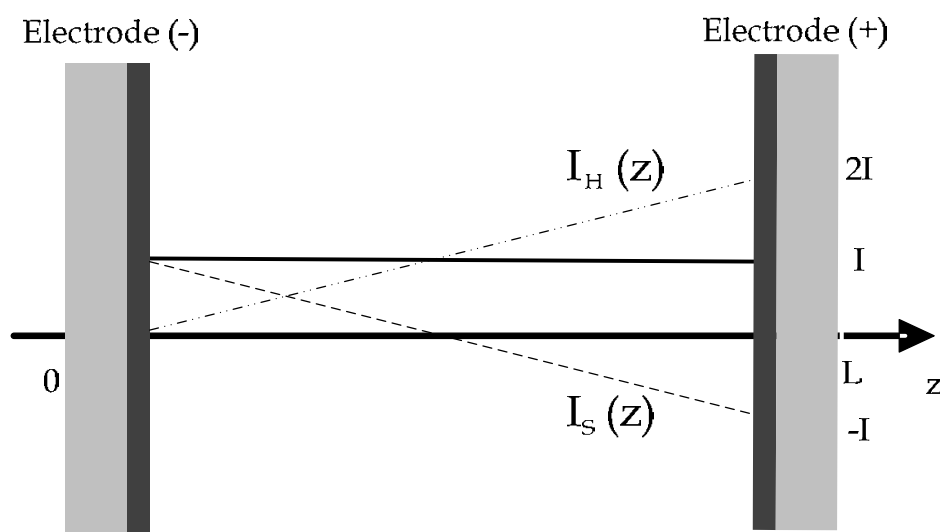


Fig. 3. Linear model of current  $I_S(z)$  et  $I_H(z)$

#### Main steps in diffusion phenomena analysis

The mains steps in our analysis will be the following:

- The total current is equal to the sulfate ion current at the negative electrode (see equation 3.a)
- Sulfate ion motion is dominated by diffusion (see next section)
- According to b), we will establish that there is a linear relationship between sulfate concentration and density current (through linear Partial Derivative Equations)
- The Nernst cell voltage may be expressed as a non linear function of the sulfate concentration for  $z=0$  (section 3.2.1.3)

As a consequence, for given boundary conditions, from a) and c) we deduce that there exists a relation of linear filtering between the total current  $I(t)$  and the sulfate anode concentration  $n_s(0,t)$ .

According to d), we find that the cell voltage  $V(t)$  may be directly expressed as a (non linear) logarithmic function of this concentration (sect 3.1.3). We propose a linearization of the problem, by the use of an exponential mapping on  $V(t)$ : in this way we introduce a "pseudo-potential" proportional to the sulfate concentration (sect 3.2.1.3). This pseudo-potential is then related to the current by linear impedance. This impedance may be simplified in terms of a RC network (3.2.2.4).

### 3.2.1.2 Diffusion fields and currents

In the electrolyte, the carriers are transported under the influence of an electric field  $E$  and the diffusion field  $\xi$ , connected to the concentration gradient. For the two types of carrier ( $k$ : Boltzmann constant;  $e$ : charge of one electron):

$$\begin{aligned}\xi_S &= -\frac{kT}{q_S} \frac{1}{n_S} \frac{dn_S}{dz} \\ \xi_H &= -\frac{kT}{q_H} \frac{1}{n_H} \frac{dn_H}{dz}\end{aligned}\quad (4)$$

Note that, from the relation:  $q_S = -2q_H = -2e$ , and the neutrality condition, we get the relation between concentrations:  $n_H = 2 n_S$ . By substitution in (4), we derive the corresponding relation between the diffusion fields:

$$\xi_H / \xi_S = q_S / q_H = -2 \quad (5)$$

The corresponding expression of the currents, for each type of carrier, is then given by the relation:

$$\begin{aligned}J_S &= \mu_S q_S n_S (E + \xi_S) \\ J_H &= \mu_H q_H n_H (E + \xi_H)\end{aligned}\quad (6)$$

In this relation,  $J_H$  and  $J_S$  have a similar magnitude (see fig 3). The mobility of hydrogen ions being much higher than the sulfate ions, this implies that  $E + \xi_H$  is very small, so that:  $E \approx -\xi_H$ . From this result and (5), we find that the current densities may be expressed in terms of the diffusion field  $\xi_S$  alone:

$$E \approx -\xi_H = 2 \xi_S \quad E + \xi_S \approx 3 \xi_S$$

Whence

$$J_S = \mu_S q_S n_S (3 \xi_S) \quad (7a)$$

Or, according to (4):

$$J_S(z) = 3 \mu_S kT \left( \frac{dn_S}{dz} \right) \quad (7b)$$

And from (2):

$$J = J_S(0) = 3 \mu_S kT \left( \frac{dn_S}{dz} \right)_0 \quad (7c)$$

This establishes the step c) of our diffusion analysis exposed in section 3.2.1.1

We may introduce in (7b) the linear profile of the current, valid in the stationary case. We then derive a parabolic symmetric profile of the concentration of sulfate ions (Fig. 4), with  $n_S(0) = n_S(L)$ .



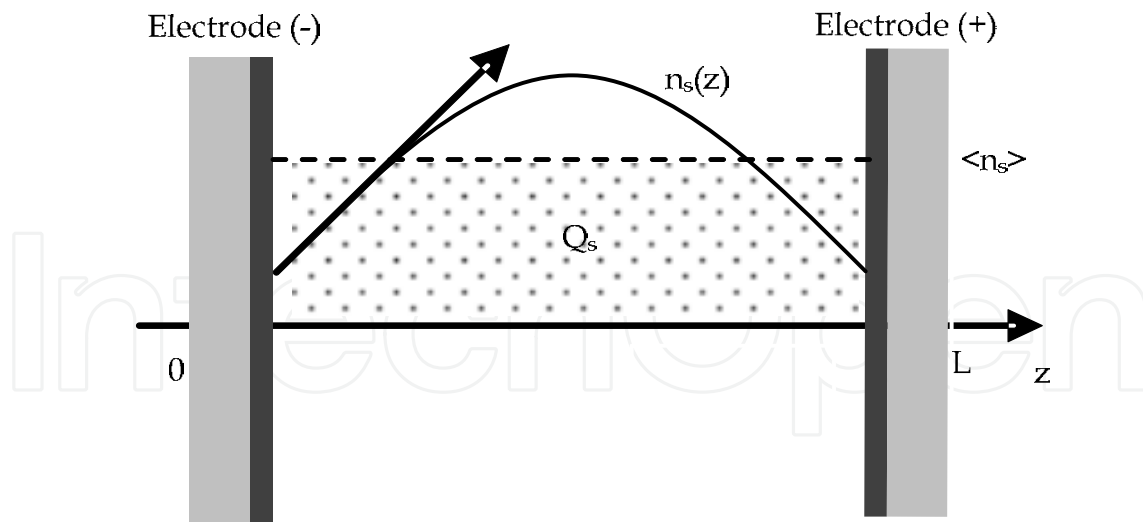


Fig. 4. Concentration profile (Stationary 1D Model)

Let us point out this symmetry property which will generalize for the dynamical case. Following the boundary condition (3a and 3b) we find:

- For currents, the **anti symmetry** property:  $I_s(L-z) = -I_s(z)$
- For densities, the **symmetry** property:  $n_s(L-z) = n_s(z)$

### 3.2.1.3 Voltage and concentration

According to the electrochemical model defined above, while applying Nernst's equation (Marie-Joseph, 2003); we obtain the expression of voltage as a function of the limit concentrations in the form:

$$V = A_1 + \frac{kT}{2e} \ln \left( \frac{n_s(0)}{a_{\text{PbSO}_4}(0)} \right) + \frac{kT}{2e} \ln \left( \frac{n_s(L)n_H(L)^4}{a_{\text{PbSO}_4}(L)} \right). \quad (8a)$$

In this relation, we may use the fact that:

- According to the neutrality condition (section 3.2.1.2),  $n_H = 2n_s$
- Due to the symmetry of concentrations,  $n_s(L) = n_s(0)$ .
- Concerning  $\text{PbSO}_4$  activity, it is equal to one, unless we are very close to full charge (this will not be considered here).

In such conditions, the expression of battery voltage may be set in the form:

$$V = A_2 + \frac{3kT}{e} \ln(n_s(0)) \quad (8b)$$

Let  $n_0$  be a reference sulfate concentration and  $E_0$  the corresponding Nernst voltage, then the relation may be written in the form:

$$\begin{cases} V = E_0 + V_L \ln \left( \frac{n_s(0)}{n_0} \right) \\ V_L = \frac{3kT}{e} \end{cases} \quad (8c)$$



This result corresponds to point *d*) in introduction (3.2.1.1).

### 3.2.1.4 “Linearised” pseudo-voltage using an exponential transformation

We suggest to introduce a “pseudo-voltage” which is a linear function of the concentration, and which aims to the voltage  $V$  when it is close to the reference voltage  $E_0$ , according to figure 5:

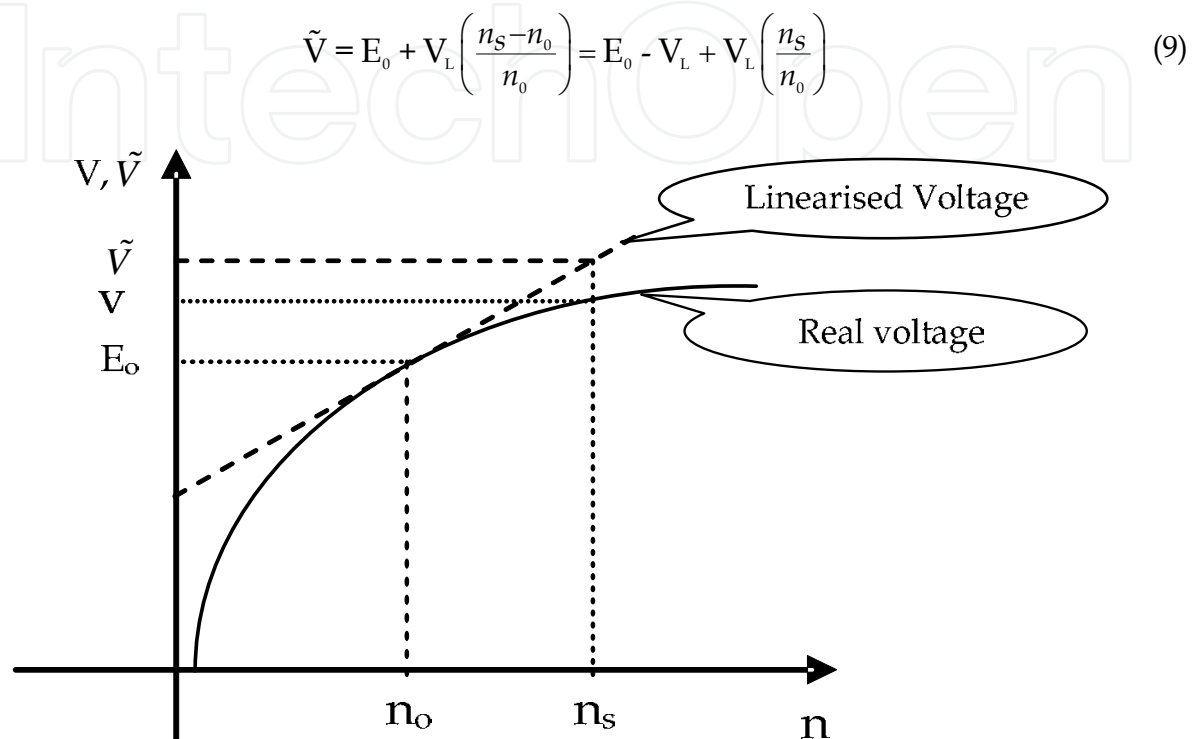


Fig. 5. Linearised Pseudo-voltage

The pseudo voltage may then be obtained by an exponential transformation of the original voltage according to the expression:

$$\tilde{V} = E_0 + V_L \left( \exp \left( \frac{V - E_0}{V_L} \right) - 1 \right) = E_0 - V_L + V_L \left( \exp \left( \frac{V - E_0}{V_L} \right) \right) \quad (10)$$

### 3.2.1.5 Constant current equivalent circuit

According to figure 4, the limit concentrations (for  $z=0$  and  $z=L$ ) are easily expressed, and may be related to the total stored charge  $Q_s$  and the internal current  $I$ :

$$\begin{cases} n_s(0) = n_s(L) = \langle n_s \rangle - \frac{L}{6} \left( \frac{dn_s}{dz} \right)_0 \\ Q_s = SL \langle n_s \rangle \\ I = I_s(0) = SJ_s(0) = 3S\mu_s kT \left( \frac{dn_s}{dz} \right)_0 \end{cases} \quad (11)$$

According to equations (8) and (11), the voltage may be expressed in terms of the stored charge  $Q_s$  and the internal current  $I$  according to:

$$\begin{cases} V = E_0 + \frac{3kT}{q} \ln\left(\frac{Q_s - \theta I}{Q_0}\right) \\ \theta = \frac{L^2}{18\mu_s kT} \end{cases} \tag{12}$$

Relation (12) may be written in terms on an RC model valid only for constant current charge or discharge in the form:

$$\tilde{V} = V_L \frac{(Q_s - \theta I)}{Q_0} = \frac{Q_s}{C_D} - R_D I \tag{13}$$

With  $C_D = Q_0/V_L$  and  $R_D = \theta/C_D$

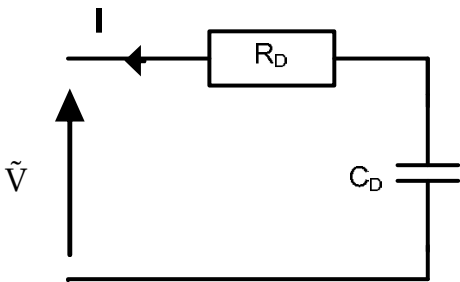


Fig. 6. RC equivalent circuit for constant current (after linearization)

3.2.2 Dynamical model for time varying current

3.2.2.1 General diffusion equations (one dimension)

In the general case, current densities and concentrations densities depend both on  $z$  and  $t$ . Equation (7) may be written in term of partial derivative:

$$\frac{\partial n_s}{\partial z} = \frac{J_s}{3\mu_s kT} \tag{14}$$

We may add the charge conservation equation:

$$\frac{\partial J_s}{\partial z} = -\frac{\partial \rho}{\partial t} = 2e \frac{\partial n_s}{\partial t} \tag{15}$$

These two coupled Partial Derivative Equations define the diffusion process (Lowney et al., 1980). The driving condition is given by relation:

$$J_s(0,t) = J(t) = \frac{I(t)}{S} \tag{16}$$

And the bounding condition resulting of the current anti symmetry:

$$J_s(L,t) = -J_s(0,t) \tag{17}$$

### 3.2.2.2 General electrical capacitive line analogy

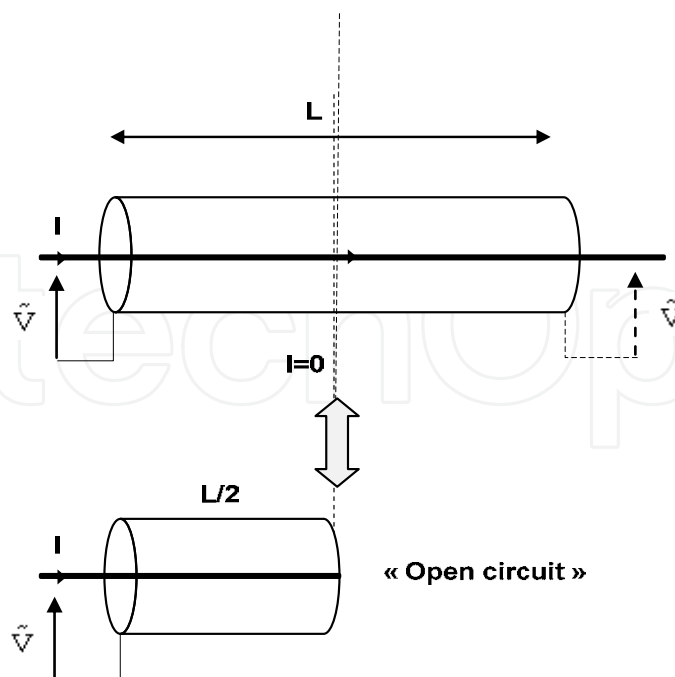
In the diffusion equations (14) et (15), making use of relation (9), the sulfate ion density  $n_s$  may be expressed in terms of the pseudo potential  $\tilde{V}$ , and the current densities  $J_s$  may be replaced by currents  $I_s = S J_s$ . We then obtain a couple of joint partial derivative equations between the pseudo voltage  $\tilde{V}(z,t)$  and the sulfate current  $I_s(z,t)$ :

$$\begin{cases} \frac{\partial \tilde{V}_s}{\partial z} = \frac{V_L}{n_0} \frac{\partial n_s}{\partial z} = \frac{V_L}{n_0 \mu_s kT} \left( \frac{I_s}{S} \right) \\ \frac{\partial I_s}{\partial z} = S \frac{\partial J_s}{\partial z} = 2eS \left( \frac{n_0}{V_L} \frac{\partial \tilde{V}_s}{\partial t} \right) \end{cases} \quad (18a)$$

These are the equations of a capacitive transmission line with linear resistance  $\rho$  and linear capacity  $\gamma$  as defined below. (Bisquert et al., (2001).

$$\begin{aligned} \frac{\partial V_s}{\partial z} &= \rho I_s & \rho &= \frac{1}{\mu_s e S n_0} \\ \frac{\partial I_s}{\partial z} &= \gamma \frac{\partial V_s}{\partial t} & \gamma &= \frac{2en_0 S}{V_L} \end{aligned} \quad (18b)$$

Taking in account the symmetry of the concentrations, we obtain an equivalent circuit consisting in a length  $L$  section of transmission line, driven on its ends with symmetric voltages. The current is then 0 in the symmetry plane at  $L/2$ . The input current is the same as for a  $L/2$  section with open circuit at the end.



(Open circuit capacitive transmission line of length  $L/2$ )

Fig. 7. Equivalent electrical circuit for the pseudo-voltage

### 3.2.2.3 Equivalent impedance solution

For linear systems, we look for solutions in the form  $A \exp(pt)$  for inputs, or  $A(z) \exp(pt)$  along the line,  $p$  being any complex constant.

Let:

$$\begin{cases} I(z, t) = I(z) \exp(pt) \\ V(z, t) = V(z) \exp(pt) \end{cases} \quad (19)$$

Then we obtain the simplified set of equations

$$\begin{cases} \frac{dV_s}{dz} = \rho I_s \\ \frac{dI_s}{dz} = \gamma p V_s \end{cases} \quad (20)$$

Whence  $\frac{d^2 I_s}{dz^2} = \rho \gamma p I_s$

Let  $\rho \gamma = \tau/L^2$ . Then  $-\alpha$  and  $\alpha$  be the solutions of :

$$\alpha^2 = p \rho \gamma = p \frac{\tau}{L^2} \quad (21)$$

Then solution for  $I_s(z)$  is a linear combination of  $\exp(\pm \alpha z)$ . If we impose  $I_s(L/2) = 0$ , then

$$I_s(z) = I_{sh} \left( \alpha \left( z - \frac{L}{2} \right) \right) \quad (22)$$

Whence:

$$V_s(z) = \frac{1}{\alpha} \rho I_{sh} \left( \alpha \left( z - \frac{L}{2} \right) \right) \quad (23)$$

We then get the Laplace impedance at the input of the equivalent circuit:

$$Z(p) = \frac{V_s(0)}{I_s(0)} = \frac{\rho}{\alpha \operatorname{th} \left( \frac{\alpha L}{2} \right)} \quad (24)$$

if  $|\alpha L| \ll 1 \quad \operatorname{th} \left( \frac{\alpha L}{2} \right) \approx \frac{\alpha L}{2}$

$$\begin{cases} Z(p) \approx \frac{1}{Cp} \\ C = \frac{\gamma L}{2} \end{cases} \quad (25)$$

In case of harmonic excitation ( $p = j\omega$ ) this corresponds to small frequencies ( $\omega\tau \ll 1$ ). The impedance is the global capacity of the line section. In practice for batteries (Karden et al., 2001), this corresponds to very small frequencies ( $10^{-5}\text{Hz}$ )

$$\text{if } |\alpha L| \gg 1 \quad \text{th}\left(\frac{\alpha L}{2}\right) \approx 1$$

$$Z(p) \approx \sqrt{\frac{\rho}{\gamma}} p^{-1/2} \quad (26)$$

In case of harmonic excitation ( $p = j\omega$ ) this corresponds to high enough frequencies ( $\omega\tau \gg 1$ ) the impedance is the same as for an infinite line (Linden, D et al., 2001), corresponding to the Warburg impedance.

#### 3.2.2.4 Approximation of the Warburg impedance in terms of RC net

An efficient approximation of a  $p^{-1/2}$  transfer function is obtained with alternate poles and zeros in geometric progression. In the same way, concerning Warburg impedances an efficient implementation (Bisquert et al., 2001) is achieved by a set of RC elements in geometric progression with ratio  $k$ , as represented in figure 8.

Let  $\omega_0 = 1/RC$ . Note that the progression of the characteristic frequencies is in ratio  $k^2$ .

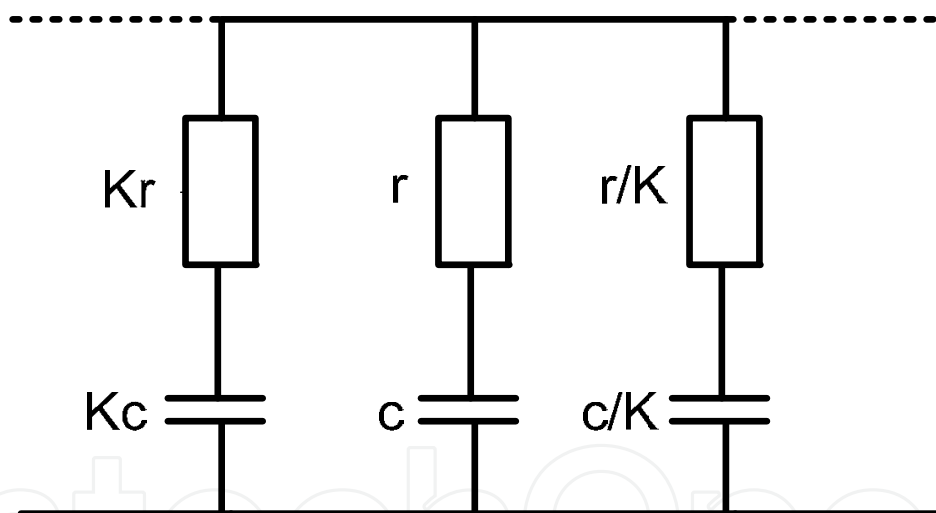


Fig. 8. RC cells in geometric progression

Let  $Y(\omega)$  be the admittance of the infinite net. It is readily verified that

- For  $\omega = \omega_0$ ,  $Y(\omega_0)$  may be set in the form  $Sk/(1-j)$ , with real  $Sk$  (complex angle exactly  $\pi/4$ )
- $Y(k^2 \omega_0) = k Y(\omega_0)$  (Translation of one cell in the net)

It can be verified by simulation that the fitting is quite accurate, even for values up to  $k=3$ .

#### 3.2.3 Approximation of a finite line in terms of RC net

The simplest approximation would to use a cascade of  $N$  identical RC cells simulating successive elementary sections of line of length  $\Delta L = L/2N$ . with:  $r = \rho \Delta L$  and  $c = \gamma \Delta L$

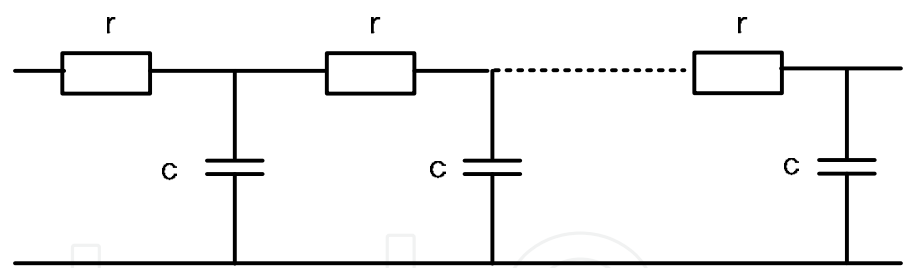


Fig. 9. Elementary approximation by a cascade of identical RC cells

This approximation introduces a high frequency limit equal to the cutoff frequency of the cells  $f_N = 1/2\pi rc$ . Drawing from the previous example concerning Warburg impedance, we propose to use  $(M+1)$  cascaded sections but with impedance in geometric progression.

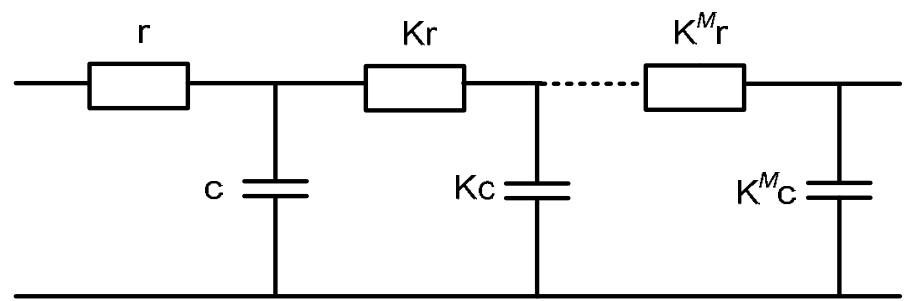


Fig. 10. Approximation by a cascade of RC cells in geometric progression

The total capacity will be equal to the total  $L/2$  line capacity. The frequency limit for the approximation remains given by the first cell cutoff frequency.

For instance for  $k = 3$  this may result in a drastic reduction of the number of cells for a given quality of approximation.

3.2.4 Practical RC model used for experimentations

In practice, the open circuit line model will be valid only if the entire electrolyte is between the cell plates. In practice this is usually not true. For our batteries, about one half of the electrolyte volume was beside the plates. In such case there is an additional transversal transport of ions, with still longer time constants. This could be accommodated by an additional RC cell connected at the output of the line.

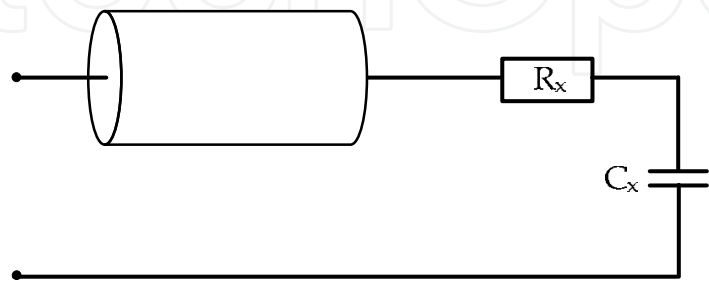


Fig. 11. Transmission line with additional RC cell

Satisfactory preliminary results for model validation were obtained with a much simplified network, with an experimental fitting of the component values (Fig 11).

We may consider that  $c$  and  $c_1$  ( $c \ll c_1$ ) account for the transmission line impedance, while  $C_x$ ,  $R_x$  ( $C_x$  in the order of  $C_1$ ) accounts for external electrolyte storage.

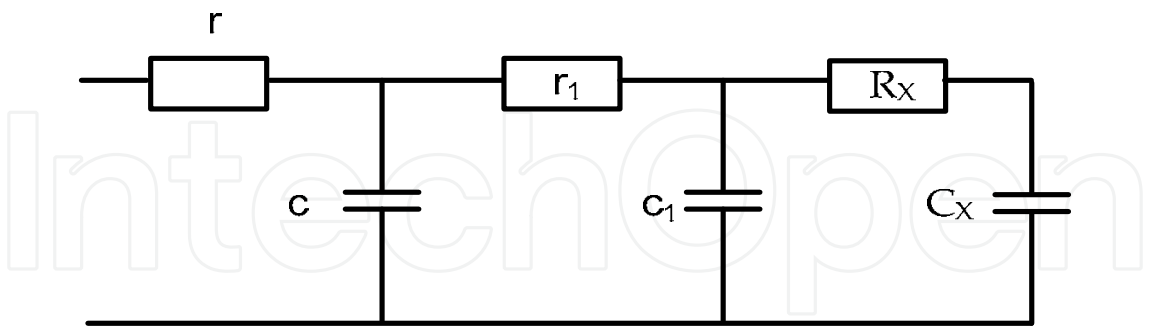


Fig. 12a. Diffusion/storage model -1-

Provided that  $C_D \ll C_1$  connection as a parallel RC cell should not modify drastically the resulting impedance. This model was introduced in order to separate “short term” and “long term” overvoltage variations in the experimental investigation.

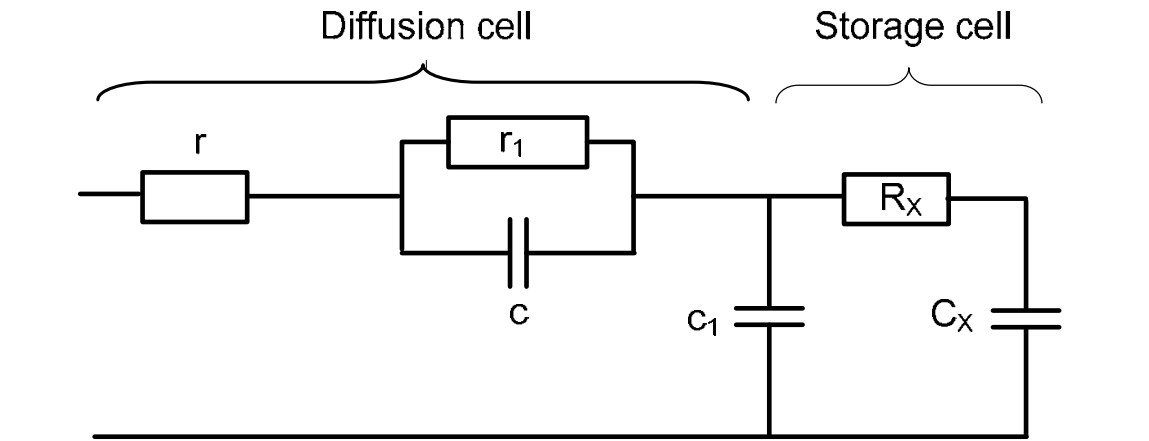


Fig. 12b. Diffusion/Storage model -2-

4. Activation voltage

4.1 Comparison to PN junction

A PN junction is formed of two zones respectively doped N (rich in electrons: donor atoms) and P (rich in holes: acceptor atoms). When both N and P regions are assembled (Fig. 13), the concentration difference between the carriers of the N and P will cause a transitory current flow which tends to equalize the concentration of carriers from one region to another. We observe a diffusion of electrons from the N to the P region, leaving in the N region of ionized atoms constituting fixed positive charges. This process is the same for holes in the P region which diffuse to the N region, leaving behind fixed negative charges. As for electrolytes, it then appears a double layer area (DLA). These charges in turn create an electric field that opposes the diffusion of carriers until an electrical balance is established.



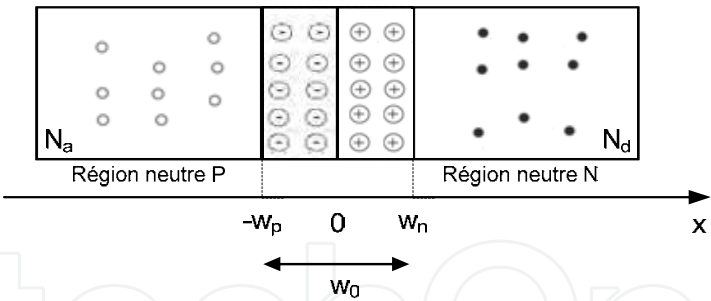


Fig. 13. Representation of a PN junction at thermodynamic equilibrium

The general form of the charge density depends essentially on the doping profile of the junction. In the ideal case (constant doping “ $N_a$  and  $N_d$ ”), we can easily deduce the electric field form  $E(x)$  and the potential  $V(x)$  by application of equations of electrostatics (Sari-Ari et al.,2005). In addition, the overall electrical neutrality of the junction imposes the relation:

$$N_aW_n = N_dW_p$$

(27)

with  $W_n$  and  $W_p$  corresponding to the limit of DLA on sides N and P respectively (Fig. 13). It may be demonstrated that according to the Boltzmann relationship, the corresponding potential barrier (diffusion potential of the junction) is given by:

$$V_0 = U_T \ln \left( \frac{N_a N_d}{n_i^2} \right), U_T = \frac{kT}{e}$$

(28)

where  $n_i$  represents the intrinsic carrier concentration. On another hand, note that the width of the DLA may be related to the potential barrier (Mathieu H, 1987). The PN junction out of equilibrium when a potential difference  $V$  is applied across the junction. According to the orientation in figure 14, the polarization will therefore directly reduce the height of the potential barrier which becomes  $(V_0-V)$  resulting in a decrease in the thickness of the DLA. (Fig. 14)

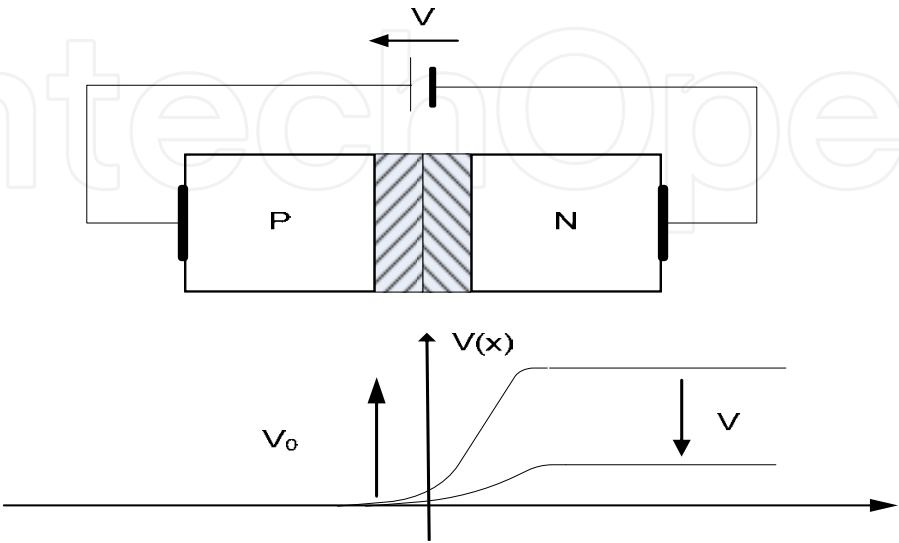


Fig. 14. Representation of a PN junction out of equilibrium thermodynamics

The decrease in potential barrier allows many electrons of the N region and holes from the P region to cross this barrier and appear as carriers in excess on the other side of the DLA. These excess carriers move by diffusion and are consumed by recombination. It is readily seen that the total current across the junction is the sum of the diffusion currents, and that these current may be related to the potential difference  $V$  in the form (Mathieu H, 1987):

$$J = J_s \left( \exp \left( \frac{V}{U_T} \right) - 1 \right) \quad (29)$$

where  $J_s$  is called the current of saturation.

On the other hand the diffusion current is fully consumed by recombination with time constant  $\tau$ , so that the stored charge  $Q$  may be expressed as  $Q = \tau J$ . This expression will be used for the dynamic model of the diode.

#### 4.2 Comparison of PN junction and electrochemical interface

From the analysis of PN junction diodes, following similarities can be cited in relation to electrochemical interfaces (Coupan and al., 2010):

- The electrical neutrality is preserved outside an area of "double layer" formed at the interface electrode / electrolyte.
- In the neutral zone, conduction is predominantly by diffusion.
- The voltage drop located in the double layer zone is connected to limit concentrations of carriers by an exponential law (according to the Nernst's equation in electrochemistry, the Boltzmann law for semi-conductors).

However, significant differences may be identified:

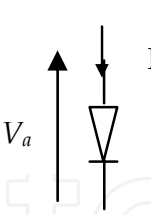
- For the PN junction, it is the concentration ratio that leads to predominant diffusion current for the minority carriers by diffusion. For lead acid battery, it is the mobility ration that explains that  $SO_4^{2-}$  ions move almost exclusively by diffusion
- There is no recombination of the carriers in the battery. As a result, in constant current operation the stored charge builds up linearly with time, instead of reaching a limit value proportional to the recombination time.
- The diffusion length is in fact the distance between electrodes, resulting in very long time constants (time constants even longer if one takes into account the migration of ions from outside the plates).
- within the overall "double-layer", additional "activation layers" build up in the presence of current, corresponding to the accumulation of active carries close to the reaction interface.

Based on method for modeling the PN junction, and the comparison seen above, we propose to analyze and model the phenomenon of activation in a lead-acid battery.

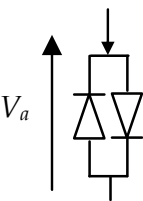
#### 4.3 Phenomenon of non-linear activation

The activation phenomenon is characterized by an accumulation of reactants at the space charge region. This electrokinetic phenomenon obeys to the Butler-Voltmer: exponential variation of current versus voltage, for direct and reverse polarization (Sokirko Artjom et al., 1995). Dynamical behavior can be introduced using a "charge driven model", familiar for PN junctions, connected to an excess carrier charge  $Q$  stored in the activation phenomenon. Bidirectional conduction can be accommodated using two antiparallel diodes. Based on the

for one single PN junction, the static and dynamic modeling of a diode is given by the current expression:


$$\begin{cases} I_{st} = J_s \left( e^{\left( \frac{V_a}{v_0} \right)} - 1 \right) = \frac{Q}{\tau_0} \\ I = \frac{Q(t)}{\tau} + \frac{dQ}{dt} \end{cases} \tag{30}$$

with Q representing an amount of stored charge and a time constant  $\tau$  associated. It is noted that one can easily model the current through the diode with an equivalent model of stored charge; this approach is valid for one current direction and not referring to the battery charge. We must therefore provide a more complete model that can be used in charge or discharge. This analysis therefore reflects a model with two antiparallel diodes. The static and dynamic modeling of the two antiparallel diodes is given by the current expression (simplified symmetric model):


$$I_{st} = G(V_a) = J_s \operatorname{sh} \left( \frac{V_a}{v_0} \right) \tag{31}$$

The static relation corresponds to the Butler Volmer equation (symmetric case). It is completed by the charge driven model:

$$\begin{cases} Q = \tau I_{st} = \tau G(V_a) \\ I = I_{st} + \frac{dQ}{dt} \end{cases} \tag{32}$$

After an analysis resulting static (and dynamic) and an experimental validation, we get the model of the phenomenon of activation with a parallel non linear capacitance and conductance circuit (fig.15) whose expressions are given by the following equations:

$$I_{st} = G(V_a) = \frac{J_0}{v_0} \operatorname{sh} \left( \frac{V_a}{v_0} \right) \text{ and } Q(V_a) = \frac{c_0}{v_0} \operatorname{sh} \left( \frac{V_a}{v_0} \right) \tag{33}$$

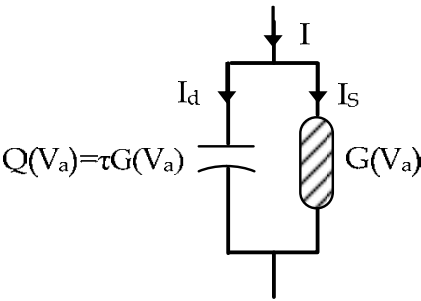
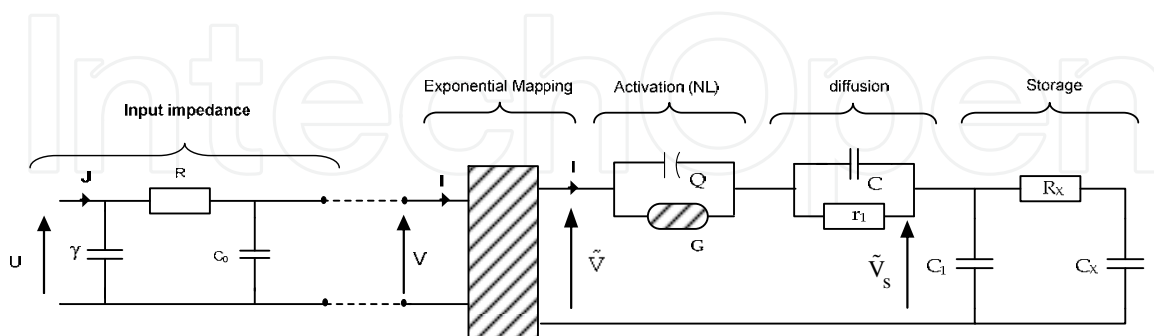


Fig. 15. Activation model : non-linear capacitance and conductance

## 5. Overvoltage model and experimental validation

By combining models obtained (diffusion phenomena/Storage, activation and input cell) and experimental measurements, we propose a simple and effective model of the battery voltage.



( $R \approx 2.5 \cdot 10^{-3} \Omega$ ,  $\gamma = 400 \text{ F}$ ,  $C_0 = 2.3 \cdot 10^4 \text{ F}$ ,  $c = 3.2 \cdot 10^4 \text{ F}$ ,  $r_1 = 2.5 \cdot 10^{-3} \Omega$ ,  $c_1 = C_x = 5 \cdot 10^5 \text{ F}$ ,  $R_x = 0.01 \Omega$ )

Fig. 16. Overvoltage model of lead acid battery

### 5.1 Experimental analysis

Identification of a linear model may be delicate, but there are a lot of classical well trained methods for this.

For a non linear system, it is difficult to find a general approach.

For most cases, it is possible to separate steady state non linear set point positioning, then local small signal linear investigation.

For battery, the set point should be defined by the state of charge and the operating current. But the fact that when you apply a non zero operating current, the state of charge is no longer fixed. This is an important practical problem, all the more critical as there is a strong dependence of the activation impedance with respect to the current. The experimental methodology presented is centered on this non linearity topic.

### 5.2 Separation on the basis of the time constant

Our objective is to establish the static value of the activation voltage as a function of current. The problem is that if the current scanning is too slow the variation of the state of charge will corrupt the measure. In such condition we can never reach the static value. Typical results are given in fig 17, compare to charge driven dynamical models as discussed in section 4.

### 5.3 Correction of battery voltage connected to the state of charge

A first hypothesis is that for slowly varying current the voltage drift is a function of the stored charge  $Q$ , computed by summation of the current. 3D plots are made as a function of the couple  $I, Q$ , with current steps to identify the relaxation time and asymptotic value as representative of the storage voltage or activation steps. (Fig.18)

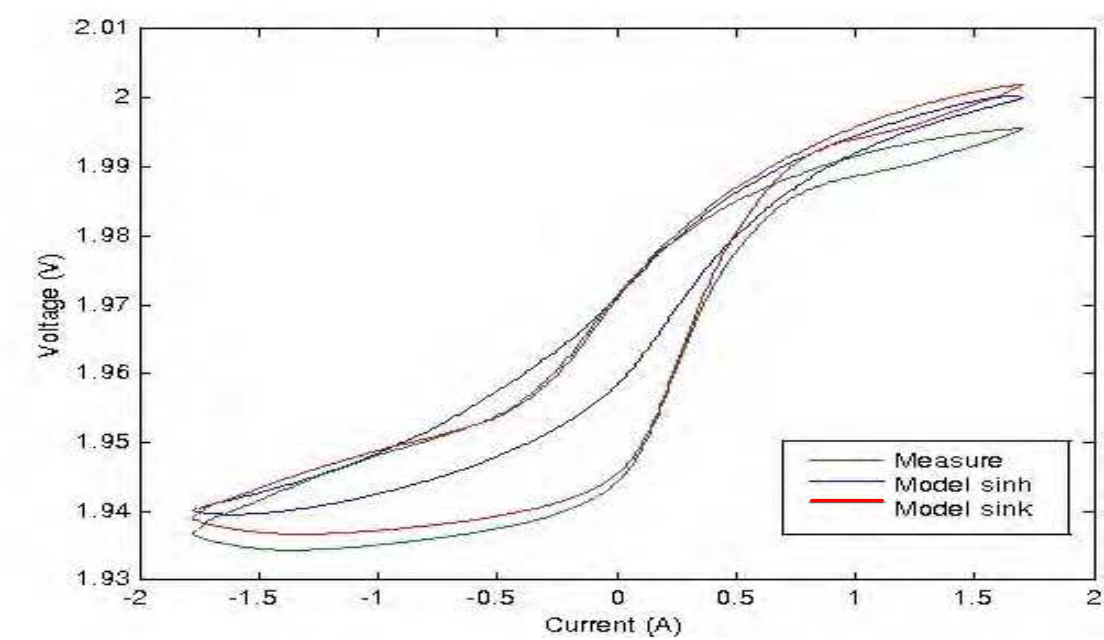


Fig. 17. Experimental analysis and simulation of activation phenomena

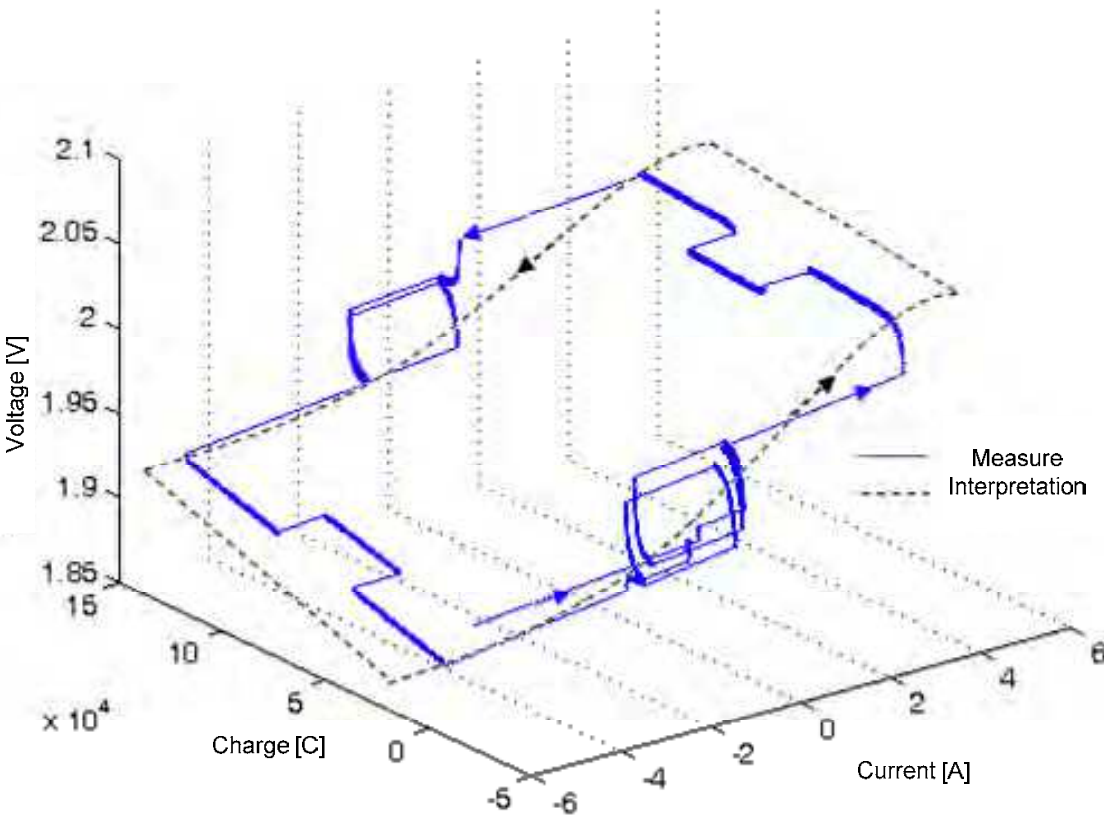


Fig. 18. Highlight of the diffusion and activation process

5.4 Improved storage voltage estimation

Instead of using  $Q$  as a reference for the storage voltage, we use the voltage given by the optimized RC storage net. Again the plot is made for steps between constant values of the current. We can see that between curves corresponding to two given values of the current, there remains a variation of the activation voltage.

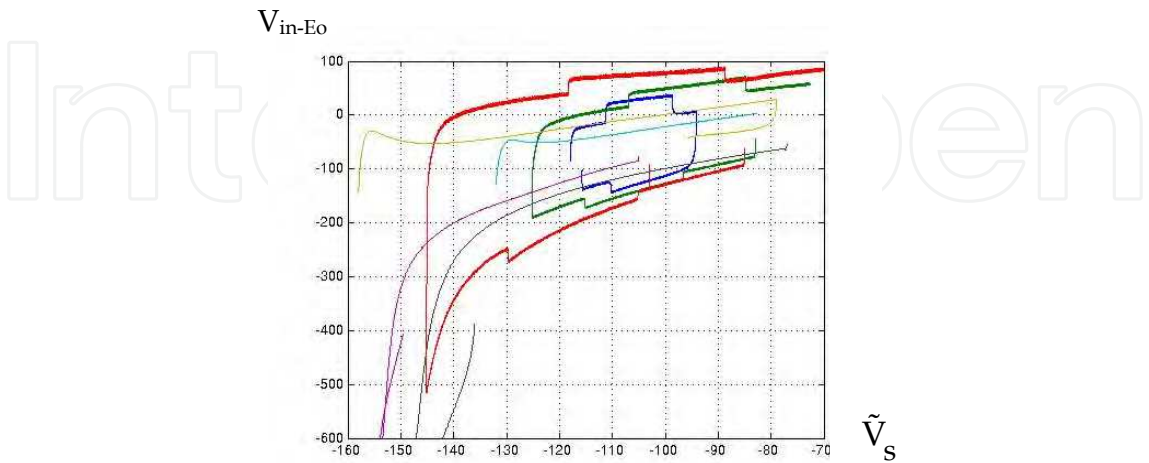


Fig. 19a. General Validation of diffusion/stockage and activation phenomena

5.5 Effect of the non linear voltage transformation

The same points are plotted using the pseudo-voltage after exponential transform. We see that now the plot between two given values of the current, which constitutes a good validation of the non linear model.

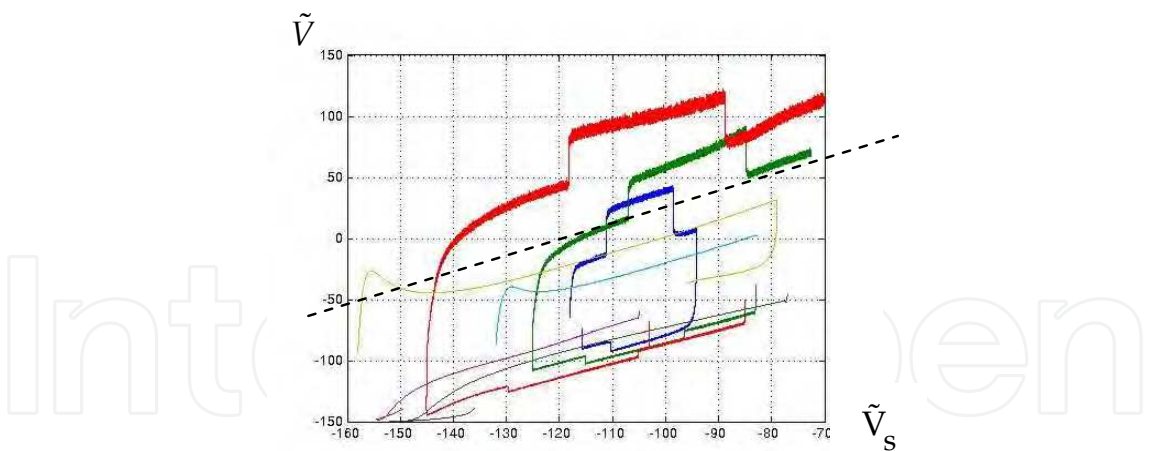


Fig. 19b. Reduction of activation voltage variations by linearisation

6. Conclusion

Electrochemical batteries are becoming quite usual components for electrical engineers. One of our purposes was to provide a good understanding for such users, by the way of a short form equivalent circuit. This equivalent circuit sums up the different steps of a simplified physical analysis. Two most important aspects may be cited:



- Investigation of nonlinearities
- Efficient lumped model for diffusion

### 6.1 Investigation of nonlinearities

Characterization of dynamical non linear systems is quite complex. Purely phenomenological description may lead to a huge number of parameters for imperfect results.

From our physical analysis, nonlinearities are summarized by two simple elements:

- The exponential mapping of voltage into a “pseudo-voltage” proportional to ionic concentration. Diffusion processes may then be described in terms of linear equivalent impedance
- The activation overvoltage, described in static by Butler Volmer equations, for which we propose a dynamical model drawing from an analogy with semiconductor diodes (charge driven model with given relaxation time)

### 6.2 Efficient lumped model for distributed parameters systems

For non specialists, the “Warburg impedance” may look a very esoteric electrochemical topic. We introduce an analogy with a subject quite trivial for electronic engineers, capacitive transmission lines. Approximation of such distributed parameter device by lumped RC network has been the subject of a lot of papers (Kuhn et al., 2006 and Mauracher et al., 1997). We propose an efficient approximation with RC cells in geometric progression.

### 6.3 Possible extensions

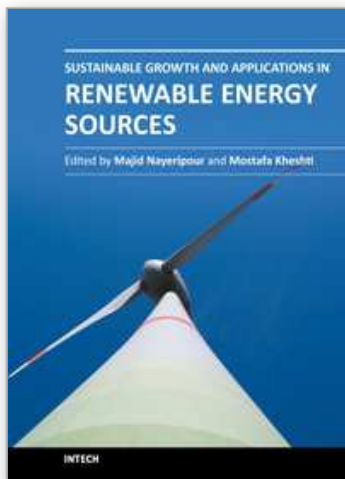
We consider that our analysis constitutes an important contribution to the understanding of battery operation, in particular for electronic engineers. It opens the way for inclusion in efficient control of complex systems, either in the field of power managing or signal processing.

## 7. References

- Bard A. (2000). *Electrochemical Methods, Fundamental and Applications*, 2<sup>nd</sup> ed., Harris D., (Ed), John Wiley & Sons, ISBN 0-471-04372-9.
- Bisquert, J.,Compte, A. (2001). Theory of the electrochemical impedance of anomalous diffusion, *Journal of Electroanalytical Chemistry*, vol. 499, pp. 112-120.
- Blanke, H., Bohlen, O., Buller S., De Doncker, R.W. Fricke, B., Hammouche, A., Linzen, D., Thele, M., et Sauer ,D.U. (2005), “Impedance measurements on lead-acid batteries for state-of-charge, state-of-health and cranking capability prognosis in electric and hybrid electric vehicles,” *Journal of Power Sources*, vol. 144, pp. 418-425.
- Coleman, M.; Chi Kwan Lee; Chunbo Zhu; Hurley, W.G.(2007). State-of-Charge Determination From EMF Voltage Estimation: Using Impedance, Terminal Voltage, and Current for Lead-Acid and Lithium-Ion Batteries, *IEEE Transactions on Industrial electronics*, Vol. 54, pp. 2550 - 2557.
- Coupan F., Sadli I., Marie-Joseph I., Primerose A., Clergeot H.(2010). New Battery dynamic Model: Application to lead-acid battery, *The 2nd International conference on computer and automation Engineering. Electrical and energy systems of IEEE volume 5* pp 140-145, Singapore, 26-28 Feb, 2010.



- Esperilla J., Félez J., Romero G., Carretero A.(2007). A model for simulating a lead-acid battery using bond graphs, *Simulation Modelling Practice and Theory*, vol. 15, pp. 82-97, 2007.
- Garche J., Jossen A., Döring H.(1997). The influence of different operating conditions, especially overdischarge, on the lifetime and performance of lead/acid batteries for photovoltaic systems, *Journal of Power Sources*, vol. 67, pp. 201-212, 1997
- Henri Mathieu, Dunod, ISBN 2-10-048633-0 (1987), *Physique des semi-conducteurs et composants électroniques*.
- Karden, E.; De Doncker, R.W.(2001). The non-linear low-frequency impedance of lead/acid batteries during discharge, charge and float operation, *Telecommunications Energy Conference, 2001. INTELEC 2001. Twenty-Third International*, pp. 65-72.
- Kuhn, E., Forgez, C., Lagonotte, P., Friedrich, G. (2006). Modelling Ni-mH battery using Cauer and Foster structures, *Journal of power sources*, vol. 158, pp. 1490-1497.
- Landolt D.(1993). *Corrosion et chimie de surfaces des métaux*, Traite des matériaux, Presses Polytechniques et Universitaires Romandes, 1993.
- Linden, D. and Reddy, T.B. McGraw-Hill, ISBN 0-07-135978-8 (2001). *Handbook of Batteries*.
- Lowney, J.R.; Larrabee, R.D. (1980). Estimating the state of charge of a battery, *IEEE Transactions on Electron Devices*, Vol. 27, pp. 1795-1798.
- Manwell Jams F., McGowan Jon G. (2003). Lead acid battery storage model for hybrid energy systems, *Solar Energy*, vol. 50, pp. 399-405, 2003
- Marie-Joseph, I., *Diagnostic methodology applied to preventive maintenance units of electricity production in isolated sites*, PhD Thesis, Université des Antilles et de la Guyane 2003.
- Marie-Joseph I., Clergeot H., Oukaour A., Linguet L. (2004). Dynamic model of an electrochemical accumulator, *19th European Photovoltaic Solar Energy Conference and Exhibition Proceeding*, 2004.
- Mauracher, P., Karden, E. (1997). Dynamic modeling of lead/acid batteries using impedance spectroscopy for parameter identification, *Journal of power sources*, vol. 67, pp. 69-84.
- Riffonneau Y., Barruel F., and Bacha S.(2008). Problématique du stockage associé aux systèmes photovoltaïques connectés au réseau, *Rev. Energ. Ren*, vol. 11, pp. 407-422, 2008
- Sari-Ari I., Benyoucef B., et Chikh-blel B.(2005). Etude de la jonction PN d'un semi-conducteur a l'équilibre thermodynamique, *Journal of Electron Devices*, vol. 5, pp.122-126,
- Sokirko Artjom, V., Bark Fritz, H.,(1995). Diffusion-migration transport in a system with butler-volmer kinetics, an exact solution, *electrochimica Acta*, vol. 40, pp. 1983-1996.



## **Sustainable Growth and Applications in Renewable Energy Sources**

Edited by Dr. Majid Nayeripour

ISBN 978-953-307-408-5

Hard cover, 338 pages

**Publisher** InTech

**Published online** 02, December, 2011

**Published in print edition** December, 2011

Worldwide attention to environmental issues combined with the energy crisis force us to reduce greenhouse emissions and increase the usage of renewable energy sources as a solution to providing an efficient environment. This book addresses the current issues of sustainable growth and applications in renewable energy sources. The fifteen chapters of the book have been divided into two sections to organize the information accessible to readers. The book provides a variety of material, for instance on policies aiming at the promotion of sustainable development and implementation aspects of RES.

### **How to reference**

In order to correctly reference this scholarly work, feel free to copy and paste the following:

Frédéric Coupan, Ahmed Abbas, Idris Sadli, Isabelle Marie Joseph and Henri Clergeot (2011). Structural Design of a Dynamic Model of the Battery for State of Charge Estimation, Sustainable Growth and Applications in Renewable Energy Sources, Dr. Majid Nayeripour (Ed.), ISBN: 978-953-307-408-5, InTech, Available from: <http://www.intechopen.com/books/sustainable-growth-and-applications-in-renewable-energy-sources/structural-design-of-a-dynamic-model-of-the-battery-for-state-of-charge-estimation>

**INTECH**  
open science | open minds

### **InTech Europe**

University Campus STeP Ri  
Slavka Krautzeka 83/A  
51000 Rijeka, Croatia  
Phone: +385 (51) 770 447  
Fax: +385 (51) 686 166  
[www.intechopen.com](http://www.intechopen.com)

### **InTech China**

Unit 405, Office Block, Hotel Equatorial Shanghai  
No.65, Yan An Road (West), Shanghai, 200040, China  
中国上海市延安西路65号上海国际贵都大饭店办公楼405单元  
Phone: +86-21-62489820  
Fax: +86-21-62489821

© 2011 The Author(s). Licensee IntechOpen. This is an open access article distributed under the terms of the [Creative Commons Attribution 3.0 License](https://creativecommons.org/licenses/by/3.0/), which permits unrestricted use, distribution, and reproduction in any medium, provided the original work is properly cited.

IntechOpen

IntechOpen